

LoopStack: a Lightweight Tensor Algebra Compiler Stack

Bram Wasti*
Meta AI

José Pablo Cambroneró†
MIT, Meta AI

Benoit Steiner
Meta AI

Hugh Leather
Meta AI

Aleksandar Zlateski*
Meta AI

Abstract

We present LoopStack, a domain specific compiler stack for tensor operations, composed of a frontend, LoopTool, and an efficient optimizing code generator, LoopNest. This stack enables us to compile entire neural networks and generate code targeting the AVX2, AVX512, NEON, and NEONfp16 instruction sets while incorporating optimizations often missing from other machine learning compiler backends.

We evaluate our stack on a collection of full neural networks and commonly used network blocks as well as individual operators, and show that LoopStack generates machine code that matches and frequently exceeds the performance of in state-of-the-art machine learning frameworks in both cases. We also show that for a large collection of schedules LoopNest’s compilation is orders of magnitude faster than LLVM, while resulting in equal or improved run time performance. Additionally, LoopStack has a very small memory footprint – a binary size of 245KB, and under 30K lines of *effective* code makes it ideal for use on mobile and embedded devices.

1 Introduction

The availability of massive amounts of computing power has fueled the explosive growth of machine learning techniques for almost a decade and has greatly affected the design of modern hardware. Companies, such as NVIDIA with their tensor cores, Intel/AMD with their specialized AVX, FMA, and VNNI instructions, ARM with the Neon and SVE extensions to their instruction set, and Apple with their M1 CPU and its matrix coprocessor, have tailored the computational capabilities of their respective hardware to better serve the needs of deep learning workloads.

However, leveraging the raw computational power of such hardware for the purpose of fast execution of machine learning models remains a challenge. Several approaches have been proposed over time, but they all suffer from significant shortcomings.

The first approach is to rely on libraries of optimized primitive tensor operations, such as cuDNN [9], OneDNN [12], or XNNPACK [16]. Unfortunately this approach has three main

downsides. First, to cover an ever growing set of use cases, these libraries tend to be large in codesize, which hinders their utilization on many devices, such as smartphones or IoT devices. Second, their development and maintenance require large amounts of manpower. Third, operators can only exchange data through global memory, which can be a significant bottleneck, especially in the case of low arithmetic intensity operators such as the activation functions.

To avoid these problems, another approach pioneered by projects such as Halide [42] and TVM [7] represent tensor computations, such as the ones underlying deep learning, using a declarative domain specific language. This high-level representation is then scheduled and lowered into LLVM intermediate representation, and then compiled into instructions that can be executed directly on hardware by the LLVM compiler. However this approach suffers from very large compilation times, thus making certain techniques, such as fast auto-tuning impractical.

To overcome these limitations, we introduce LoopStack, a lightweight toolchain designed specifically for deep learning workloads. To express computations, LoopStack introduces a **domain specific representation** based on Einstein’s notation. This representation can capture many common dense neural network operations in a concise form. LoopStack also provides a **frontend** capable of converting neural networks, expressed as dataflow graphs, into our representation. Finally, we present a **code generator** that can extremely quickly convert this representation into highly optimized code for X86 and ARM CPUs.

Unlike other approaches that rely on off-the-shelf components such as LLVM, LoopStack was designed from the ground up to target machine learning workloads. This enables our system to make the following contributions:

- Milliseconds compile times, a fraction of time compared to traditional compilers.
- Performance comparable to or exceeding that of hand-optimized libraries such as MKL-DNN or XNNPACK.
- Small code footprint resulting in a lightweight binary.

2 Tensor Contractions

Tensor operations, such as inner, outer, and cross product, as well as matrix multiplication, trace, transpose, and many other tensor operations can be expressed as special cases

*Corresponding authors: {bwasti,zlateski} at fb dot com.

† Author contributed while interning with Meta and completing studies at MIT.

of contraction. In fact, with a few extensions, contractions can encode all the operations that the most popular deep neural networks rely on. We demonstrate how to express computations over tensors as generalized contractions. We also discuss the challenges inherent in optimizing (aka scheduling) these contractions.

2.1 Generalized Tensor Contractions

Before introducing generalized, d -dimensional tensor contractions, we first present a simple example in 2-dimensions – the matrix multiplication operation. Figure 1 demonstrates two different, though equivalent, ways that describe the matrix multiplication operation. The imperative pseudocode in Figure 1a shows the typical set of 3 nested for-loops iterating over dimensions i and j of the output matrix (C) and the *reduction dimension* k . Note the reduction over k is explicit in this notation.

In the tensor index (Einstein) notation [13, 33, 43] (Figure 1b), the i and j index variables appear on both the left- and right-hand side of the formula indicating that in order to compute the corresponding entry in C we index A and B with the same values of i and j . The index variable k , represents a reduction variable, as it appears solely on the right-hand side the formula. In particular, the for-loop over varying values of k for a specific assignment to i and j , and the corresponding aggregation (i.e. contraction), is left implicit. Similarly, the for-loops over varying values of i and j , needed to populate C , are left implicit.

We use generic \oplus and \otimes notation to emphasize that different operators can be used to instantiate a generalized matrix *multiplication* operation.

```

for i:
  for j:
    C[i, j] = alpha * C[i, j];
    for k:
      C[i, j] += beta * A[i, k] * B[k, j]

```

(a) Pseudocode for basic imperative matrix-multiplication.

$$C_{i,j} = \alpha C_{i,j}^{in} \oplus \beta (A_{i,k} \otimes B_{k,j})$$

(b) Equivalent declarative Einstein notation for matrix multiplication, with $\oplus = +$ and $\otimes = *$.

Figure 1. Matrix multiplication

We can generalize the matrix-multiplication example to d -dimensions, where our inputs are now d -dimensional tensors, to result in *tensor contractions*. Following notation presented in [15], let A , B , and C now be d -dimensional tensors (for potentially different d). Let the set of dimensions for A , B , and C be denoted by I_A , I_B , and I_C , respectively. Let I_{AC} be the dimensions of C present in A , while I_{AR} are

reduction dimensions¹ in A . Similarly I_{BC} are dimensions of C present in B , while I_{BR} are reduction dimensions in B . We now write:

$$C_{I_C} = \alpha C_{I_C}^{in} \oplus \beta (A_{I_{AC} \cup I_{AR}} \otimes B_{I_{BC} \cup I_{BR}})$$

We further extend this notation to allow indexing into a tensor to be an affine transformation of the indices.

Finally, we extend our notation to allow for an element-wise operation that initializes the output tensor (*pre-operation*) and an element-wise operation that can transform a value before final storage into the output tensor (*post-operation*). We can now write

$$C_{(I_C)} = \text{post}(\text{pre}(C_{f_C}^{in}) \oplus \beta (A_{f_A(I_{AC} \cup I_{AR})} \otimes B_{f_B(I_{BC} \cup I_{BR})}))$$

where f_C , f_A and f_B are affine transformations and pre/post are the element-wise pre- and post- operations. These concepts are useful for expressing biases and activation functions in machine learning workloads.

With these extensions, we can not only express GEMM, GEMV, and GEVM operations, but many more operations as well. Such as:

- Convolutions – $O_{r,c} = I_{r+k,c+j} \cdot \omega_{k,j}$
- pooling – $O_{r,c} = \max(I_{2r+k,2c+k})$
- reductions – $O_r = I_{r,c}$
- transpositions – $O_{r,c} = I_{c,r}$
- concatenations – $O_{r,c'} = I_{r,c'}^1; O_{r,|c'|+c''} = I_{r,c''}^2$
- broadcast – $O_{r,c} = I_r$

2.2 Optimizing Generalized Contractions

The way we carry out these generalized contraction computations has a significant impact on performance. For example, a naive 3-nested for-loop implementation of matrix multiplication of figure 1a will result in long running times for non-trivially sized matrices. In contrast, efficient implementations, as proposed by many researchers over the past few decades [17, 19, 29, 35, 40, 45, 63], might modify the imperative loops to tile (i.e. split into sub-matrices of appropriate sizes) the input matrices to align with architecture-dependent resources such as cache sizes, re-order loop dimensions to re-use data in the innermost loop, exploit architecture features such as vector instructions to operate on multiple elements at a time, and emit extended instructions such as fused-multiply-add, which combine multiplication and accumulation at the instruction level. Further, the data might be kept in *exotic* memory layouts, such as the channel-interleaved format often used on Intel machines [12, 64], or the matrix tile interleaved format proposed by Jia et al. [29, 63].

Typical scheduling operations include: re-ordering, splitting, fusing, parallelizing, vectorizing, and unrolling loops [18,

¹Dimensions contracted by a user-defined operation, such as the shared dimension of the input matrices in a matrix multiplication.

42]. The scheduling options for a single task such as matrix-multiplication highlight the combinatorial challenge underlying scheduling. Different computations and platforms require varying schedules to deliver performance gains. This results in a challenging optimization problem. Historically, varying techniques have been put forward to tackle this optimization, ranging from expert-based manual optimization, analysis-driven heuristic optimization [18, 36], to recent advances in data-driven automated schedule exploration [2, 7]

In the remainder of this paper, we introduce both the frontend (LoopTool) and backend (LoopNest) of LoopStack as well as a TUI for manual tuning and a script for automatic tuning built on top of LoopStack.

3 LoopStack Design

LoopStack is composed of a frontend (LoopTool) and a backend (LoopNest). This design separates the representation of the program being described from the logic to emit target-specific code.

The frontend (LoopTool) is designed to enable expression of both the user’s mathematical intent (a chain of extended tensor contractions) as well as the preferred execution of the program – the order in which basic mathematical operations should be executed (i.e. the schedule) to perform the desired tensor contraction. This is done by defining a structured intermediate representation composed exclusively of a dataflow graph (DFG) as well as a loop order annotation language that denotes how each node is executed. The omission of control flow in the representation of the program is consistent with a large majority of neural network, which can be well represented as purely functional operations on N-dimensional tensors. The design of this IR – the design of our DFG, as well as the loop order annotations, is explained thoroughly in section 4.

The backend, LoopNest, is designed to generate optimized machine-code efficiently that strictly adheres to the user’s input. LoopNest exposes an API that allows the user to define a specific loop nest order in which the computation should be performed; LoopNest will not make any attempt to change the provided nest order or use any logic to recover user intent. In short – LoopNest will generate machine code that performs the exact computation that the user requested, and in the same order. However LoopNest will attempt to apply all known low level optimizations that are relevant to the target hardware, such as loop unrolling[28, 30, 31, 46, 54, 59, 60], vectorization [10, 28, 31, 46, 60], reordering of independent instructions [10, 28, 30, 31, 46, 53, 59], software pipelining [10, 28, 31, 46, 53, 59], minimizing the amount of auxiliary operations. More about LoopNest code generation and optimizations is discussed in section 5.

3.1 Design principles and goals

3.1.1 Simplicity

The goal of simplicity extends to both the description of intended mathematical operations and the language of defining the execution order (the schedule) of the resultant loops.

We use an Einstein-like notation [13] embedded in Python, described in 4, as it allows the user to easily describe the intended mathematical operations even for complex machine learning models. For instance, defining a multi layer perceptron (MLP), which is often used for NLP [], recommendation [] models, etc., can be achieved as seen in in the Listing 1.

```
HL1[b, i] += W1[i, j] * Input[b, j]
Act_1[b, i] = lt.relu(HL1[b, i])
HL2[b, k] += W2[k, i] * HL1[b, i]
# ...
Out[b] = lt.sigmoid(WN[o, p] * HLN[b, p])
```

Listing 1. MLP defined with our Einstein notation-like syntax

We provide a minimal IR and limit the API such that almost all optimization operations can be decomposed into a series of operations on individual nodes in the DFG. Wrappers are provided to manipulate nodes in bulk (e.g. to change the loop order of both the multiplication and the addition in a matrix multiplication at once), yielding an interface similar to Halide’s pipeline scheduling states[2]. However, unlike in Halide, it is impossible to represent illegal schedules in our IR. We discuss the optimizations in detail in section 6.

There are only a handful of global optimization parameters, such as the unroll limit and the parameters describing the target hardware, most of which are encoded inside the LoopNest.

3.1.2 Performance Predictability & Fast Feedback

Traditional compilers perform expensive analysis in order to understand user intent and optimize execution, while performing equivalent computation. This approach has two major drawbacks. First, the user does not get accurate feedback about the quality of their intended schedule of execution; and second, the compilation time is significantly increased due to expensive analysis. LoopStack takes a different approach. Once the user annotates the IR, no layer in LoopStack attempts to understand the user’s intent and/or reorder the intended schedule provided by the user, except in very few, hardware-specific cases. Currently, these cases only include reordering mathematical operations inside the innermost unrolled loop. Such optimizations have relatively minor effect on the overall performances – they increase the utilization of the underlying hardware by a few percentage points, but also allow the user to squeeze the last bits of the available computational power. In addition, such optimizations highly

```

import loop_tool as lt
M, N, K = lt.Var("m"), lt.Var("n"), lt.Var("k")

A = lt.Tensor([M, K])
B = lt.Tensor([K])
C = lt.Tensor()

C[m, n] += A[m, k] * B[k]

```

Figure 2. LoopTool’s Python embedded declarative DSL

depend on the limitations of the target hardware, and are not easy to expose to the user.

This approach allows LoopStack to perform extremely fast compilation (on the order of milliseconds), as well as allow the user to understand the quality of their intended schedules and rapidly explore scheduling ideas. In addition, this approach can greatly benefit autotuning [2, 61] algorithms by leveraging both the predictability and efficiency of benchmarking schedules.

4 Frontend (LoopTool)

In order to allow users to effortlessly describe the desired computation of neural network workloads using LoopStack, we built a domain specific language (DSL) embedded in Python and a compiler front-end that we termed LoopTool. LoopTool exposes a declarative API for user definition of computation and operates on an IR composed of an annotated dataflow graph (DFG) consisting of N-dimensional tensor operations. The DFG describes the underlying computation, memory layouts and execution. LoopTool then lowers the DFG into a series of loops, which are then compiled with LoopNest.

4.1 Declarative API

Figure 2 shows an example of matrix multiplication in LoopTool’s declarative Python DSL. The expression `lt.Var("m")` defines an indexing variable with the corresponding name. Next, the expression `lt.Tensor([M, K])` defines a 2-dimensional tensor. Note that LoopTool uses symbolic (i.e. named) dimensions [44], which simplify indexing semantics and encourages a simple interaction model for manipulating traversal and memory layouts of higher dimensional tensors. The expression `C[m, n] += A[m, k] * B[k]` defines computation using the aforementioned tensor (Einstein) notation; here `k` is a reduction dimension. LoopTool’s computation language supports element-wise computations (with broadcast semantics), associative reductions across arbitrary dimensions, and a restricted set of indexing semantics (see Section 4.2.3).

4.2 Intermediate Representation (IR)

LoopTool’s DFG is based on an intermediate representation with annotations on each node. Each node is associated with its output – a virtual buffer that is materialized according to the user provided schedule. Figure 3 (left) demonstrates a

matrix multiplication without annotations. A node’s output size is not materialized until the IR is lowered to loops. The materialization logic always attempts to minimize the total memory used. For example, two nodes operating on virtual buffer of size N in a shared loop over N do not need to allocate the full N elements of memory for their intermediate. Instead, the intermediate will be of size 1 and reused N times. This can be seen in Figure 3.

LoopTool’s DFG has three fundamental types of nodes.

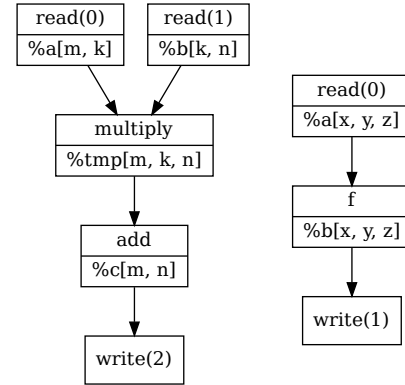


Figure 3. Matrix multiplication in LoopTool (left). A point-wise application of the function f across all three dimensions of $\%a$ (right).

4.2.1 Read/write nodes

Read and write nodes denote reads or writes from and into user provided memory, as well as associated layouts and sizes. These nodes contain an ordered list of symbolic dimensions. The ordered list of dimensions represents a row-major order (lexographical order) of either input or output memory. Because LoopStack is embedded in either Python or C++ applications, these nodes are used to interface with other operations that are not handled by LoopStack. An example would be the specification of NCHW[41] or NHWC[1] layouts for the inputs to convolution operations, both of which are well handled and trivially manipulated in the LoopTool IR. In the IR, read nodes take no inputs whereas write nodes take a single input and have no outputs. These are fundamentally source and sink operations in the graph.

4.2.2 Arithmetic nodes

Arithmetic nodes operate on virtual buffer and output a single virtual buffer. The ordered list of dimensions associated with these nodes denotes how output memory should be laid out (given the corresponding scope of their execution).

Arithmetic nodes, unlike read and write nodes, can take multiple inputs. This represents the typical operation applied to the inputs. For example, addition of two inputs works as expected to yield a single output.

Extending this concept to higher dimensions forces us to consider when two inputs do not have the same dimensions. Due to the symbolic nature of the dimensions in LoopTool, we can distinguish two dimensions of the same size as being mathematically distinct. To handle application of arithmetic in higher dimensions we employ implicit broadcasting akin to Numpy[39] semantics. Dimensions not present in the output are implicitly reduced over according to the arithmetic of the associated node.

4.2.3 View nodes

The final type of node admits the representation of symbolic indexing constraints over tensor dimensions, allowing powerful view semantics. Any affine combination of iteration over the output dimensions can be used to index into an input dimension. This enables us to represent windowed operations as well as concatenations. By using index constraints rather than index equations, we preserve the meaning of the underlying computation and can freely split and permute variables and layouts. Further, by keeping indexing math symbolic, we can still apply the scope based memory minimization logic.

4.3 Lowering to loops

LoopTool lowers its IR to an internal loop tree structure before invoking LoopNest. This is done by traversing the DFG topologically and eagerly emitting loops that are required for each node. A reference to the current innermost loop is maintained throughout this entire process, with each subsequent loop nesting inside the reference. If any node requires a loop that is an ancestor to the current reference, there is no need to emit the loop again (it would be incorrect to do so) and it is skipped. This naturally induces loop coalescing (typically referred to as loop fusion).

Consider nodes shown in Figure 3 (right). We can assume an annotation of %a and %b both with loop order [x, y, z]. When visiting %a's node, we emit the loop tree shown in Listing 2.

Later, while visiting %b's node, we note that the reference (which is at location %a) contains a loop for x, y, and z in order. We thus reuse all loops and implicitly "fuse" node %b. This is shown in Listing 3.

We find the nodes can be executed in the same innermost loop. The resultant allocation size of %a would be 1 in this case.

```
iter x:
  iter y:
    iter z:
      %a[x, y, z] = read(x, y, z)
    ...
```

Listing 2. Lowering %a emits three new loops.

```
iter x:
  iter y:
    iter z:
      %a[x, y, z] = read(x, y, z)
      %b[x, y, z] = f(%a[x, y, z])
```

Listing 3. Lowering %b reuses all loops.

However, if the nodes had different loop annotations, such as %b annotated with [x, z, y], we would not be able to share every loop. The memory allocated for %a in that case would be of size $|y| \cdot |z|$. This is shown in Listing 4.

```
iter x:
  iter y:
    iter z:
      %a[x, y, z] = read(x, y, z)
  iter z:
    iter y:
      %b[x, y, z] = f(%a[x, y, z])
```

Listing 4. Only loop x is shared across the two nodes.

In the case of reductions, we cannot always share loops. Consider a reduction node %R over variable z with loop order [x, y, z] depended on by %a with the same loop order; see Listing 5. The loop for z is required to run twice for correctness. This type of behavior, while necessary for reductions, may be preferable in other contexts as well.

```
iter x:
  iter y:
    iter z:
      %R[x, y] = reduction(...)
    iter z:
      %a[x, y, z] = %R[x, y] + ...
```

Listing 5. Sharing loop z between %R and %a would be mathematically incorrect.

Manually preventing loop sharing can induce larger intermediate memory allocations. This is often beneficial when computation benefits from packing memory into cache-friendly layout before computation. To express this, LoopTool has a second form of annotation for nodes called *staging*

that prevents reuse of specific loops. In listing 3, %a and %b share an entire loop nest. If we were to *stage* the loop for %a over z, the resultant lowering would increase the allocation size of %a to |z| (Listing 6).

```
iter x:
  iter y:
    iter z:
      %a[x, y, z] = read(x, y, z)
    iter z:
      %b[x, y, z] = f(%a[x, y, z])
```

Listing 6. z is staged, so %a is materialized with an allocation of size |z|.

5 Backend (LoopNest)

LoopNest is a domain specific compiler for a series of nested loops, with user specified innermost operation. LoopNest is designed to have extremely short compilation times and use well known and studied high-performance computing (HPC) optimizations to generate high performance code.

5.1 LoopNest’s HPC Philosophy

While traditional compilers typically perform multiple optimization passes, some of which might be repeated, LoopNest’s is designed to only do a limited number of optimizations, but do them very well. These include HPC optimizations that are commonly used in expert designed, custom assembly, or code generator primitives for specific problems, such as matrix multiplications [4, 21, 22, 32, 51, 52] and other primitives used in machine learning [9, 12, 14, 20, 29, 62, 63]. Additional HPC optimization might include instruction re-ordering, r-sum, and other optimizations suggested by optimization manuals for the target hardware [3, 26].

LoopNest’s generated code directly reflects the computation requested by the user: in particular, operations are performed in user-specified order. Generating code directly from the user-defined execution order simplifies code generation logic, which results in a more intuitive mapping between the quality of the provided execution order and the observed performance of the code. In addition, the provided (high level) information about the loop order and sizes are used for LoopNest’s simple register allocation approach, described below.

While having default choices based on the target hardware manuals, LoopNest optionally delegates the choice of which loops to be unrolled. The user may override the hardware tuned default maximum number of unrolled instructions, and LoopNest will determine the outermost loop such that the number of unrolled instructions doesn’t exceed the user specified value.

Vectorization

LoopNest assumes that the user intent is to vectorize the innermost loop in the user provided schedule. This design simplifies the logic, while not introducing any limitations to the user – the elements of the vector operation are executed at the same time, thus naturally belong to the innermost loop. LoopNest will, thus, attempt to vectorize the innermost loop. However, in certain scenarios, when the data accessed inside the innermost loop is not contiguous, and the target hardware doesn’t support efficient gather operations, LoopNest will fallback to scalar operations.

No–Spilling of the Resulting Tensor

The concept of tiling (or "blocking") for the multiple levels of a cache hierarchy and the register file is a well known optimization technique [17, 19, 35, 45]; referred to as *Cache Blocking Techniques* in the Intel’s optimization manual [26]. LoopNest exposes this common HPC optimization, where the subset of the output tensor is kept in register file [12, 20–22, 29, 62, 63]. LoopNest never produces code that spills the content of the register file to the stack, an approach that is commonly used in traditional compilers, such as LLVM or GCC. Spilling the content of the register file to stack puts pressure on the hardware’s load/store units, preventing full hardware utilization.

LoopNest does not decide on blocking or tiling sizes, nor on the size used for the data kept in registers (register blocking). LoopNest instead identifies the outermost user provided loop for which the all compute can be performed with a subset of the output tensor kept in registers. Thus, it’s up to the user to provide a well chosen loop order and sizes – one where the values kept in the register file can be reused many times. This approach gives the user a greater control, with more predictable performance as compared to the case when spilling is allowed.

5.2 Single Operand LoopNest

LoopNest also provides functionality for generating efficient code for a simplified tensor contraction, where there are no reduction dimensions, and only one input is provided. This functionality is typically used for *reshaping* a tensor (such as numpy’s **reshape** function), but can also be used for extracting a subset of a tensor into a smaller tensor, or broadcasting elements along a tensor dimension. This functionality is required by LoopStack in order to allow the user’s schedules that prefer to reorganize the memory for faster access [17, 19, 35, 45]

5.3 Generalizing to computations with multiple loop nests

Some computations or their schedules can result in a sequence of multiple nested loops that may share a set of outer loops, effectively forming a tree of loops. To generalize our

approach to these workloads, we developed a loop tree interface. The loop tree interface provides a simple API to build up a tree, where inner nodes correspond to for-loops, and leaves correspond to an innermost computation over tensors or a transposition of tensors. LoopNest then compiles all independent nests and executes the tree. The final result is a function that can be called with the appropriate input, intermediate, and output tensors to realize the computation defined by the tree.

6 IR Manipulation and Optimization

6.1 Interaction Model

A core challenge in high-performance tensor operations is identifying a good execution order – the schedule. As noted previously, there can be many valid schedules for a given computation: loops can be split and reordered, dimensions can be split and swapped, intermediate tensors can be packed, and so on. As a result, any scheduling tool is faced with the challenge of an exponentially large search space making simple enumeration infeasible. Recent work [2, 61] has explored using a combination of machine learning and structured search strategies to automatically explore the search space.

While automation presents a promising direction, expert intuitions (and their use in a guided search) remain an important factor in developing high performance kernels today. As a result, a key goal of LoopStack is to facilitate exploration of schedules. Effective exploration depends on real-time feedback, which an expert can use to validate their intuitions and incrementally explore the space of possible schedules. To deliver real-time, instantaneous [38], feedback, LoopTool exploits LoopNest’s fast code generation to compile and benchmark schedules with low-latency (on the order of 10-100ms for programs not bounded by the execution of the underlying generated code).

6.2 Manual Tuning

To promote human driven exploration with LoopTool, we developed a terminal based user interface (TUI). Fig. 4 presents a matrix multiplication example using LoopTool’s visual TUI. The schedule for the computation is reflected in the TUI and provides controls to interactively manipulate the schedule, including splitting and reordering loops and memory. LoopTool can automatically benchmark the schedule presented and display statistics useful for optimization. As shown in Fig. 4, LoopTool reports the total required number of operations (FLOPs), arithmetic intensity (The ratio of FLOPs performed and memory transfers [25, 56, 56]), and the achieved performances in billions of floating point operations per second (GFLOPS). This information allows experts to iterate on kernel schedules quickly, and non-experts to ramp up on schedule and hardware performance characteristics.

The speed with which a developer can experiment with different schedules allows exploring solutions optimally tuned

```

%12[k0, n0] = in%13[k0, n0]
iter m0 over 512
  %9[m0, k0] = in%10[m0, k0]
  iter n0 over 512
    iter k0 over 512
      %6[m0, k0, n0] = %9[m0, k0] * %12[k0, n0]
      %3[m0, n0] = %3[m0, n0] + %6[m0, k0, n0]
    out%0[m0, n0] = %3[m0, n0]
  
```

```

arithmetic intensity: 341.333
total flops: 2.68435e+08
compile time: 0.699ms
achieved GFlops: 1.48144
sample outputs:
0.419777 5.5757 -4.03335 -3.65078 -8.3475 18.4119 -7.69373 -19.695 -3.89912 10.7263

```

Figure 4. Initial UI for a 512x512x512 matrix multiplication and a real-time measured performance window.

```

enter new inner size: 64

```

```

%9[m0, k0] = in%10[m0, k0]
iter n0 over 512
  %6[m0, k0, n0] = %9[m0, k0] * %12[k0, n0]
  %3[m0, n0] = %3[m0, n0] + %6[m0, k0, n0]
out%0[m0, n0] = %3[m0, n0]

```

```

%12[k0, n0, n1] = in%13[k0, n0, n1]
iter m0 over 512
  %9[m0, k0] = in%10[m0, k0]
  iter n0 over 8
    iter k0 over 512
      iter n1 over 64
        %6[m0, k0, n0, n1] = %9[m0, k0] * %12[k0, n0, n1]
        %3[m0, n0, n1] = %3[m0, n0, n1] + %6[m0, k0, n0, n1]
      out%0[m0, n0, n1] = %3[m0, n0, n1]
    
```

```

%12[k0, k1, n0, n1] = in%13[k0, k1, n0, n1]
iter m0 over 102 r2
  %9[m0, m1, k0, k1] = in%10[m0, m1, k0, k1]
  iter n0 over 8
    iter k0 over 32
      iter k1 over 16
        iter m1 over 5
          iter n1 over 64
            %6[m0, m1, k0, k1, n0, n1] = %9[m0, m1, k0, k1] * %12[k0, k1, n0, n1]
            %3[m0, m1, n0, n1] = %3[m0, m1, n0, n1] + %6[m0, m1, k0, k1, n0, n1]
          out%0[m0, m1, n0, n1] = %3[m0, m1, n0, n1]
        
```

```

arithmetic intensity: 340.888
total flops: 2.67387e+08
compile time: 14.033ms
achieved GFlops: 78.0216
sample outputs:
0.419776 5.5757 -4.03335 -3.65078 -8.3475 18.412 -7.69373 -19.695 -3.89913 10.7263

```

Figure 5. Splitting loops vastly improves performance. LoopStack gracefully handles tail logic (seen for variable m), enabling efficient 5x64 register blocking. The k loop is split to induce unrolling.

- How easy is it to extend LoopTool to support new sets of instructions?

7.1 Setup

Experiments are performed on total of 6 different CPU cores and 4 different vector extensions: Intel Xeon Platinum 8124M with the avx512 vector extension; AMD Epyc 7R32, with the avx2 vector extension; Cortex A57, Cortex A73, NVIDIA Denver 2 and Apple M1 CPUs – all with ARM’s neon vector extension; and finally, Apple M1 with the neon_fp16 vector extension. We perform all experiments single-threaded; using a single core on the target hardware, in order to analyze the contributions of our work. Using multi-threaded workloads would also depend on the underlying threading implementations, and can skew our desired measurements.

7.2 Operator Benchmarking vs Traditional Compilers

A key contribution of LoopNest, the backend of LoopStack, is the reduced compile times required for generating high performance code. To validate this contribution, we compare LoopStack to LLVM, which is a popular backend choice for existing tensor operation compilers such as Halide [42, 48] and TVM [7, 8].

Figure 1 presents 12 operator we have evaluated, consisting of matrix multiplications (fully connected layers), convolutions, and depth-wise convolutions over varying input sizes. To provide a fair comparison of LLVM and LoopStack, we evaluate both systems on the same set of schedules and perform pair-wise comparisons. For LLVM code generation, we use Halide to emit schedules identical to the ones used with LoopStack. We ensure that LLVM’s runtime assertions, as well as bound checks, are turned off. As LLVM is a general, *catch-all* compiler, performing apples-to-apples comparison is not an easy task; for that reason, we instruct LLVM to use the same optimizations as the ones used in practice – such as the ones used in Halide [2, 15, 48] and TVM [7, 8]. We focus our evaluation on two key dimensions: compile time and execution time.

We generate a set of schedules with the rule-based heuristic scheduler referred to in Section 6.3, which performs a sweep of execution schedule optimizations such as tiling. We attempt to collect schedules seen throughout this tuning process, but only collect schedules that result in a single loop nest (i.e. there are no shared outer loops across different nested inner loops). After we obtain a full set of schedules for a benchmark, we evaluate both LoopStack and LLVM on them.

Figure 2 presents a summary of compile times across benchmarks. The “LLVM” and “LoopNest (LN)” columns present the average number of milliseconds to generate machine code for schedules for the corresponding benchmark. The “ratio” columns presents the average ratio of LLVM compile time relative to LoopNest compile time. Our experiments

Operator	Sizes	Benchmark Name
GEMM	64 x 64 x 64	MM-64
GEMM	128 x 128 x 128	MM-128
GEMM	256 x 256 x 256	MM-256
GEMM	512 x 512 x 512	MM-512
Convolution	(channels:64 to 128), size:56x56, filter:3x3, stride:1	CONV-1
Convolution	(channels:128 to 256), size:28x28, filter:3x3, stride:1	CONV-2
Convolution	(channels:256 to 512), size:14x14, filter:3x3, stride:1	CONV-3
Convolution	(channels:512 to 512), size:7x7, filter:3x3, stride:1	CONV-4
Depth-wise Convolution	(channels:16), size:112x112, filter:3x3, stride:2	DWCONV-1
Depth-wise Convolution	(channels:72), size:56x56, filter:3x3, stride:2	DWCONV-2
Depth-wise Convolution	(channels:88), size:28x28, filter:3x3, stride:1	DWCONV-3
Depth-wise Convolution	(channels:240), size:14x14, filter:5x5, stride:1	DWCONV-4

Table 1. Summary of operator benchmarks for LoopNest/LLVM comparison

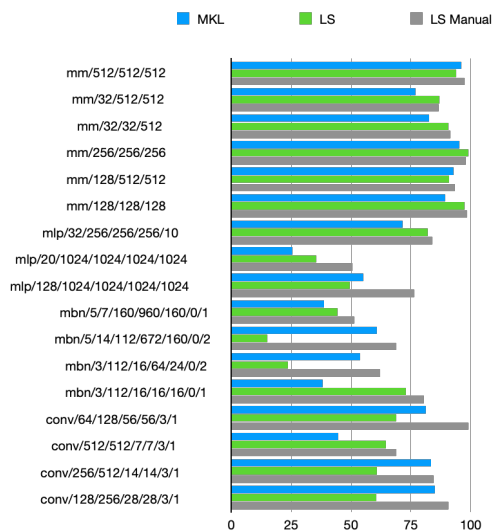


Figure 7. Comparison of MKL-DNN, Scripted, and Manual tuning using LoopTool on an AMD EPYC 7R32 CPU core using the AVX2 vector extension.

show that LoopNest’s code generation is faster than LLVM’s compilation for all schedules, all workloads and on all target hardware. In most cases LoopNest can generate code orders of magnitude faster. The significantly shorter compilation times enable use of LoopNest in automated schedule searches.

In Figure 2, we show the average run-times of the top 5 fastest schedules, for each compiler. While LLVM does outperform on some very inefficient schedules (not presented), we decide not to use slower schedules in our analysis, as such schedules will not be used in practice. Our results suggest that LoopNest is generating code that has at least comparable performances, or exceeds the performances of the one generated by LLVM – while taking just a fraction of time. Additionally, as a dependency, LoopStack’s carries only a binary of 250Kb in size, as compared to LLVM (which defaults to more than 350Mb); this makes LoopNest an obvious choice for at least mobile and embedded systems.

	x86 based CPUs						Aarch64 (ARM) based CPUs (NEON)											
	AMD (AVX2)			Intel (AVX512)			Cortex A57			NVIDIA Denver2			Cortex A73			Apple M1		
	LLVM	LN	Ratio	LLVM	LN	Ratio	LLVM	LN	Ratio	LLVM	LN	Ratio	LLVM	LN	Ratio	LLVM	LN	Ratio
CONV-1	820.78	2.5153	326.31	9881.9	6.2062	1592.3	2948.4	9.2109	320.1	3972.4	30.28	131.19	4914.6	22.077	222.61	555.24	24.763	22.422
CONV-2	1590.1	11.717	135.7	9531.3	5.8035	1642.3	2481.1	8.9475	277.29	4798.5	21.768	220.44	4310.1	31.053	138.8	531.12	15.261	34.802
CONV-3	762.52	5.9325	128.53	11061	11.411	969.29	3113.2	17.749	175.4	4184.3	24.184	173.02	3919.1	25.51	153.63	444.29	20.435	21.742
CONV-4	885.74	41.163	21.518	10706	14.264	750.56	4084.3	66.102	61.788	5169.9	85.97	60.136	6408.8	99.952	64.119	827.22	35.605	23.233
DWCONV-1	838.46	0.29416	2850.3	10551	0.28027	37647	2775.9	3.8011	730.28	4108.2	5.0464	814.09	4844.8	2.8047	1727.4	571.46	1.209	472.67
DWCONV-2	1033.8	0.47162	2192	11812	0.67874	17402	2795.3	2.5241	1107.4	3814.5	5.2036	733.06	4160.9	1.8825	2210.3	470.53	0.5241	897.79
DWCONV-3	969.88	0.30031	3229.6	13759	1.4601	9423.3	2726.6	2.158	1263.5	3666.1	4.2326	866.15	3320	3.8216	868.74	506.63	0.66237	764.87
DWCONV-4	1000.7	0.33429	2993.4	10704	0.81343	13159	3474	5.5112	630.34	4577.5	9.4771	483.01	4197.4	2.8767	1459.1	449.89	1.6	281.18
MM-64	697.37	0.38452	1813.6	9099.5	0.85309	10667	3432.4	7.3588	466.43	4779.2	13.103	364.75	4417.6	9.1708	481.7	397.59	1.3267	299.68
MM-128	925.47	1.578	586.47	9044.8	0.79484	11379	4991.9	11.153	447.57	5754.2	16.025	359.07	6681.1	13.956	478.72	387.82	1.1188	346.63
MM-256	1118.5	2.6925	415.41	18119	3.0202	5999.4	5003.1	18.511	270.28	5770.9	26.485	217.9	6800.6	27.446	247.78	390.29	5.1647	75.57
MM-512	1262.3	4.3405	290.83	12336	4.4847	2750.8	4814.2	7.4852	643.17	5698.9	12.25	465.22	6471.7	14.545	444.94	1084.4	9.5121	114

Table 2. Compile times, in milliseconds, for LLVM and LoopNest. LoopNest performs the compilation orders of magnitude faster

	x86 based CPUs						Aarch64 (ARM) based CPUs (NEON)											
	AMD (AVX2)			Intel (AVX512)			Cortex A57			NVIDIA Denver2			Cortex A73			Apple M1		
	LLVM	LN	Ratio	LLVM	LN	Ratio	LLVM	LN	Ratio	LLVM	LN	Ratio	LLVM	LN	Ratio	LLVM	LN	Ratio
CONV-1	86.767	87.638	1.01	72.943	162.48	2.2274	11.021	11.126	1.0095	10.968	14.782	1.3477	9.8466	9.3994	0.95458	98.121	97.51	0.99377
CONV-2	45.765	71.482	1.5619	13.813	156.78	11.35	11.276	11.179	0.99134	13.407	14.511	1.0824	9.8105	9.2468	0.94254	95.743	92.027	0.96119
CONV-3	9.4946	72.433	7.6289	96.448	184.4	1.9119	8.1811	10.183	1.2447	6.4069	13.27	2.0712	6.4671	7.9984	1.2368	53.681	83.252	1.5509
CONV-4	3.307	90.722	27.434	123.73	181.72	1.4687	5.3246	9.5687	1.7971	4.3611	12.532	2.8736	2.9514	7.686	2.6042	46.806	77.952	1.6654
DWCONV-1	48.695	62.541	1.2844	48	57.592	1.1998	6.3521	6.2343	0.98146	10.243	11.858	1.1577	3.9988	4.5019	1.1258	40.133	39.01	0.97201
DWCONV-2	39.203	53.465	1.3638	28.302	37.671	1.331	5.1196	5.7031	1.114	7.1075	7.9688	1.1212	2.5178	2.7729	1.1013	42.865	43.438	1.0134
DWCONV-3	62.873	84.848	1.3495	57.544	88.094	1.5309	6.9338	7.7209	1.1135	10.65	12.551	1.1785	5.7644	6.4571	1.1202	70.796	76.261	1.0772
DWCONV-4	77.071	84.21	1.0926	125.04	159.38	1.2747	9.6875	10.174	1.0502	12.665	14.717	1.1621	7.6075	8.0169	1.0538	81.588	80.901	0.99157
MM-64	85.808	102.2	1.191	144.67	187.65	1.2971	12.751	13.441	1.0541	14.039	15.754	1.1221	9.523	10.166	1.0675	91.18	199.81	2.1913
MM-128	92.692	102.5	1.1058	168.84	185.19	1.0969	12.417	12.496	1.0064	14.253	15.291	1.0728	9.2462	9.5062	1.0281	91.763	98.4	1.0723
MM-256	92.862	100.21	1.0791	170.18	182.46	1.0722	11.428	11.401	0.99761	14.241	14.645	1.0284	8.6863	8.6103	0.99125	95.597	99.902	1.045
MM-512	90.189	98.199	1.0888	160.42	159.59	0.9948	6.9971	8.3267	1.19	14.395	13.894	0.9652	6.3364	6.8905	1.0874	89.618	97.65	1.0896

Table 3. Measured execution performances, in GFLOPS, for code generated by LLVM and LoopNest. LoopNest achieves comparable (within measurement error) or superior performances, while taking a fraction of time to generate the code.

7.3 Neural Network Workload: Benchmarking vs Traditional Libraries/Frameworks

Figure 3 presents a selection of operations common in modern neural networks. In the table (as well as figures 7,8,9,10,11,12) benchmarks prefixed with "mm" are single matrix multiplications of varying size. The "mlp" workloads simulate 3-layer multi-layer perceptrons of varying batch size and hidden dimensions. These include ReLU activations after each fully connected layer and no final reduction layer. The "mobilenetV3" workloads are depth-wise separable cells taken from the MobileNetV3 model architecture [24] run with a fixed spatial dimension of 12x12 and varying channel sizes. All benchmarks are run in C++ against the most recent version of MKL-DNN [11] using PyTorch [41] for convenience, as well as the most recent version of XNNPACK [16] through TFLite [1].

We compared the performance of the best schedules generated by LoopStack using scripted tuning as described in Section 6.3. Additionally we compared performances of manually optimized schedules using the manual tuning TUI described in Section 6.2. The tuning was done by the authors by starting from the best schedules generated with the scripted

tuning, and spending no more than a dozen of minutes per schedule.

Our results show that, our simple tuning script, implemented in less than 500 lines of Python code, outperforms hand-optimized primitives in most cases; additionally our manually optimized schedules outperform the hand-tuned primitives in **all** cases. LoopStack, including the scripted tuner as well as the TUI, is implemented in fewer than 30K lines of code², whereas MKL-DNN and XNNPACK both have an order of magnitude more lines of code.

7.4 Extending LoopTool to New Hardware

Additionally, we perform a set of benchmarks on Apple's new M1 chip using the neon_fp16 extension. Extending LoopStack to support fp16 computation required a set of changes in LoopNest compiler that are specific to the new target. This changes took less than 10 engineering-days, in fewer than 1000 lines of code. In Figure 13 we show the results of scripted and manual tuning on Apple's M1 chip, which is capable of around 210 GFLOPS peak performances. Our results suggest, that with a minimal amount of expert work,

²As measured with the standard `cloc` utility

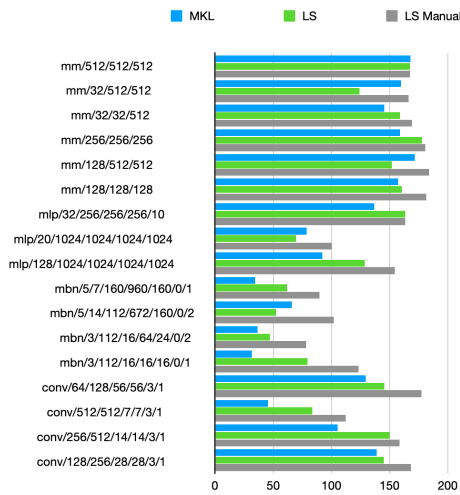


Figure 8. Comparison of MKL-DNN, Scripted, and Manual tuning using LoopTool on an Intel(R) Xeon(R) Platinum 8124M CPU core using the AVX512 vector extension.

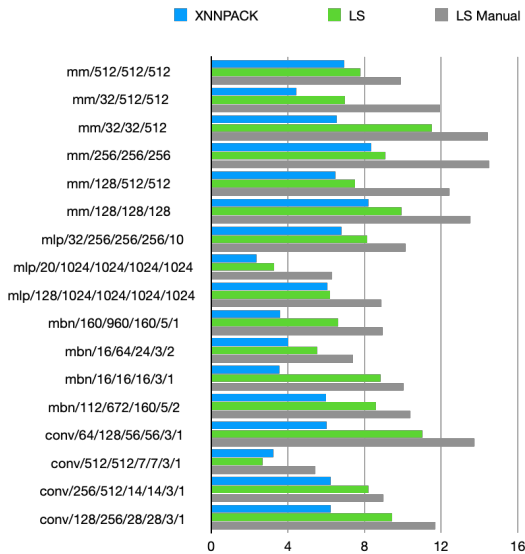


Figure 9. Comparison, in GFLOPS, of XNNPACK, Scripted, and Manual tuning using LoopTool on an ARM Cortex A57 CPU core using the neon vector extension.

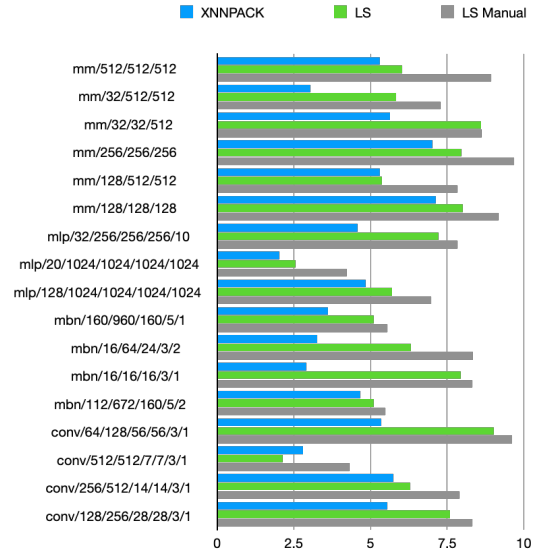


Figure 10. Comparison, in GFLOPS, of XNNPACK, Scripted, and Manual tuning using LoopTool on an ARM Cortex A73 CPU core using the neon vector extension.

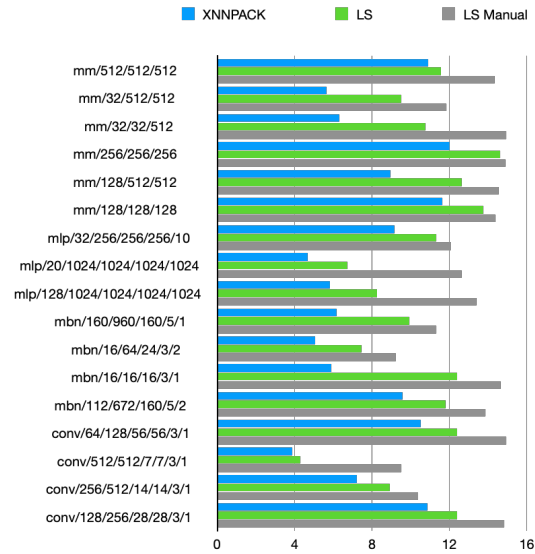


Figure 11. Comparison, in GFLOPS, of XNNPACK, Scripted, and Manual tuning using LoopTool on an NVIDIA ARM Denver 2 CPU core using the neon vector extension.

as compared to traditional, hand-optimized libraries, we can achieve extremely high utilization of new target hardware.

8 Related Work

Several alternative approaches have been proposed to efficiently execute tensor based computation on hardware. They fall in one of two broad categories: systems for high-performance tensor operations and scheduling of tensor operations.

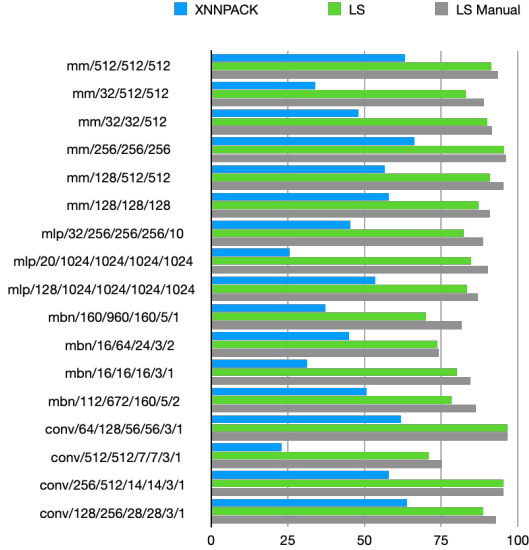


Figure 12. Comparison, in GFLOPS, of XNNPACK, Scripted, and Manual tuning using LoopTool on an Apple M1 CPU core using the neon vector extension.

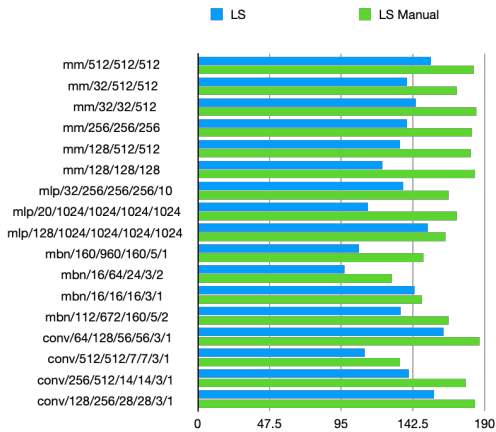


Figure 13. Results of LoopTool’s guided search, in GFLOPS, and manual optimizations using the TUI on Apple’s M1 chip (capable of around 210 GFLOPS) using neon_fp16 extension.

High Performance Tensor Operations

Intel’s Math Kernel Library (MKL) [11] provides high performance kernels for common operations such as matrix-matrix multiplications, matrix-vector multiplications, matrix decompositions, and transformations. OneDNN (previously known as MKL-DNN) [12] similarly aims to provide high performance implementations of common neural network operators such as convolution, softmax, normalization, and others, which can be composed to implement performant pipelines. In contrast to these libraries, LoopNest does not maintain separate implementations for an enumeration of different operators and sizes, rather it provides an efficient

code generation approach to support operations over arbitrary sizes/shapes. In doing so, LoopNest supports generating code for entire pipelines, rather than composing individual operators, which can be efficient independently but may otherwise result in subpar performance when composed.

Tensor-Contraction Code Generator (TCCG) [47] is a approach for performing tensor multiplication. To obtain high performance, TCCG draws on three separate approaches, and integrates them into a single tool that generates C++ code. It frames tensor multiplication as nested loops, transposition followed by use of an efficient GEMM implementation, and loops over GEMMs. In contrast to TCCG, LoopNest is not designed specifically for tensor-tensor multiplication (though it supports it), but rather provides support for additional operations and targets whole-pipeline code generation. While TCCG generates C++ code (which must then be compiled), LoopNest uses compilation to target x86 and aarch64. Finally, TCCG folds in the search for a schedule, in that it generates varied implementations (using the different techniques underlying the tool), scores them with a performance model, and then compiles the most promising ones.

Polly [18] is a polyhedral optimizer for LLVM code. Polly provides support for high-performance generalized matrix multiplication, which like LoopNest allows users to express computation with different multiplication and reduction operators. However, in contrast to LoopNest, Polly is not a standalone code generator and instead is designed to work as an optimization pass in LLVM. As we have shown in our evaluation, compiling code with LLVM is orders of magnitude slower than compiling using LoopNest.

Halide [42] and TVM [7] are compilers for general computational pipelines (with operators commonly used in image and tensor processing) and deep learning, respectively. Both allow users to implement high performance machine learning pipelines by using a declarative language to express tensor computations and a separate language for scheduling the execution of those computations. The scheduling languages support important primitives such as splitting, re-ordering, vectorizing, unrolling, or parallelizing loops, among other scheduling operations. After a computation has been scheduled, Halide and TVM use LLVM to generate executable CPU code. As a front-end, LoopTool’s use of two DSLs emulates that of Halide and TVM, and provides support for a subset of the scheduling operations. As an efficient compiler, LoopNest provides the complementary goal of efficient code generation. In particular, a goal of LoopNest is to become a viable CPU back-end alternative for systems such as Halide and TVM, enabling reduced compile times.

Schedule Exploration

Several techniques have been proposed [2, 49] to automatically schedule Halide pipelines. These approaches represent a schedule as a collection of loop nests, which are recursively optimized from the output stage back to the input. At each

step, they consider where to insert the storage and compute associated with that stage and they explore different tilings of the stage. To efficiently perform this exploration, they use search algorithms such as beam search, guided by a performance model. The performance model is a deep learning network trained to predict the runtime of a pipeline given a manually defined set of features describing the computation graph as well as the schedule.

AutoTVM [8] uses simulated annealing to produce candidate schedules, which are obtained by applying multi-level loop tiling, loop reordering, caching sub-results, and annotating loops for unrolling and vectorizing. The simulated annealing procedure relies on a cost model as a scoring function. Their cost model is instantiated to be one of various tree-learning algorithms or a neural network, which embeds the schedule directly and applies a linear layer to predict runtime cost. Similarly to [2] and [49], AutoTVM’s tree regressors rely on extracting lower-level features from the schedule such as memory access information.

Ansor [61] uses a combination of techniques to automatically schedule TVM programs. Ansor’s leverages what they term “program sketching”, where higher level scheduling templates are automatically generated by iteratively applying rule-based expansions and lower level scheduling decisions are applied as annotations. Once a complete program is sampled (by applying random annotations to a sketch), its schedule is evolved using evolutionary search and a learned cost model to identify promising candidates. These promising candidates can then be benchmarked on hardware to obtain actual performance measurements, allowing Ansor to refine its cost model for following iterations of the search.

In contrast to these systems, LoopTool was designed to provide real-time assistance to experts manually exploring schedules. LoopTool’s feedback (e.g. arithmetic intensity, compile time, GFLOPs achieved) allows developers to quickly validate their intuitions. However, while LoopTool’s design focuses on manual search, we believe LoopTool’s feedback could be used by future automated search tools. In particular, automated search tools could (due to short compile times) evaluate many more candidates through LoopTool than otherwise possible. Underlying the fast responsiveness of LoopTool is LoopNest’s ability to generate high-performance code in orders of magnitude less time than traditional backends. In a similar direction, LoopNest’s simple and fast code generation, which transparently maps the schedule provided to code generated – eschewing traditional approaches using an intermediate representation and multiple compiler passes – could facilitate extracting more meaningful schedule features for learned cost models directly from the compiled code.

9 Conclusion

We presented LoopStack, a lightweight compiler designed from the ground up for deep learning workloads. By exclusively targeting programs that can be expressed using a generalized version of Einstein’s notation, LoopStack avoids most of the complexity inherent in general purpose compilers. This enables it to compile deep neural networks several orders of magnitude faster than alternatives approaches. This also results in a much smaller code base, and therefore a much more lightweight binary ³, which can be embedded in edge devices such as IoT, sensors, and so on. Furthermore, this clarity of purpose made it implement custom optimizations that really helps the performance of the generated code. Indeed, LoopStack has proven to be extremely competitive against state of the art implementations of deep neural networks on the extensive suite of benchmark we evaluated it on.

LoopTool also exposes its schedule feedback through a simple API, allowing downstream systems to consume information on a particular schedule and update that information as incremental schedule changes are issued. This model of interaction, paired with its fast compile/benchmarking, opens up the future possibility of using LoopTool in a reinforcement learning approach, where schedule operations are “actions” that update the problem “state” (loop structure), and feedback provided by LoopTool functions a “reward” (e.g. achieved GFLOPs per second).

References

- [1] Martín Abadi, Paul Barham, Jianmin Chen, Zhifeng Chen, Andy Davis, Jeffrey Dean, Matthieu Devin, Sanjay Ghemawat, Geoffrey Irving, Michael Isard, et al. 2016. Tensorflow: A system for large-scale machine learning. In *12th {USENIX} symposium on operating systems design and implementation ({OSDI} 16)*. 265–283.
- [2] Andrew Adams, Karima Ma, Luke Anderson, Riyadh Baghdadi, Tzu-Mao Li, Michaël Gharbi, Benoit Steiner, Steven Johnson, Kayvon Fatahalian, Frédo Durand, et al. 2019. Learning to optimize halide with tree search and random programs. *ACM Transactions on Graphics (TOG)* 38, 4 (2019), 1–12.
- [3] R ARM. 2016. Cortex-A57 Software Optimization Guide. *ARM* (2016).
- [4] Sergio Barrachina, Maribel Castillo, Francisco D Igual, Rafael Mayo, and Enrique S Quintana-Orti. 2008. Evaluation and tuning of the level 3 CUBLAS for graphics processors. In *2008 IEEE International Symposium on Parallel and Distributed Processing*. IEEE, 1–8.
- [5] Henricus M Bouwmeester. 2012. *Tiled algorithms for matrix computations on multicore architectures*. University of Colorado at Denver.
- [6] Gerald G Brown. 1975. NUMERICAL PERFORMANCE OF MATRIX INVERSION. (1975).
- [7] Tianqi Chen, Thierry Moreau, Ziheng Jiang, Lianmin Zheng, Eddie Yan, Haichen Shen, Meghan Cowan, Leyuan Wang, Yuwei Hu, Luis Ceze, Carlos Guestrin, and Arvind Krishnamurthy. 2018. TVM: An Automated End-to-End Optimizing Compiler for Deep Learning. In *13th USENIX Symposium on Operating Systems Design and Implementation (OSDI 18)*. USENIX Association, Carlsbad, CA, 578–594. <https://www.usenix.org/conference/osdi18/presentation/chen>

³LoopStack is implemented in fewer than 5% lines as compared to MKL-DNN and XNNPACK, and its binary is 200x smaller than LLVM’s

- [8] Tianqi Chen, Lianmin Zheng, Eddie Yan, Ziheng Jiang, Thierry Moreau, Luis Ceze, Carlos Guestrin, and Arvind Krishnamurthy. 2018. Learning to optimize tensor programs. In *Advances in Neural Information Processing Systems*. 3389–3400.
- [9] Sharan Chetlur, Cliff Woolley, Philippe Vandermersch, Jonathan Cohen, John Tran, Bryan Catanzaro, and Evan Shelhamer. 2014. cudnn: Efficient primitives for deep learning. *arXiv preprint arXiv:1410.0759* (2014).
- [10] Marius Cornea. 2015. Intel AVX-512 instructions and their use in the implementation of math functions. *Intel Corporation* (2015), 1–20.
- [11] Intel Corporation. 2020. MKL Developer Reference. <https://software.intel.com/content/www/us/en/develop/documentation/mkl-developer-reference-c/top.html>.
- [12] Intel Corporation. 2020. OneDNN. <https://github.com/oneapi-src/oneDNN>.
- [13] Albert Einstein. 1923. Die grundlage der allgemeinen relativitätstheorie. In *Das Relativitätsprinzip*. Springer, 81–124.
- [14] Erich Elsen, Marat Dukhan, Trevor Gale, and Karen Simonyan. 2020. Fast sparse convnets. In *Proceedings of the IEEE/CVF Conference on Computer Vision and Pattern Recognition*. 14629–14638.
- [15] Roman Gareev, Tobias Grosser, and Michael Kruse. 2018. High-performance generalized tensor operations: A compiler-oriented approach. *ACM Transactions on Architecture and Code Optimization (TACO)* 15, 3 (2018), 1–27.
- [16] Google. 2020. XNNPACK. <https://github.com/google/XNNPACK>.
- [17] Kazushige Goto and Robert A van de Geijn. 2008. Anatomy of high-performance matrix multiplication. *ACM Transactions on Mathematical Software (TOMS)* 34, 3 (2008), 1–25.
- [18] Tobias Grosser, Hongbin Zheng, Raghesh Aloor, Andreas Simbürger, Armin Größlinger, and Louis-Noël Pouchet. 2011. Polly-Polyhedral optimization in LLVM. In *Proceedings of the First International Workshop on Polyhedral Compilation Techniques (IMPACT)*, Vol. 2011. 1.
- [19] John A Gunnels, Greg M Henry, and Robert A Van De Geijn. 2001. A family of high-performance matrix multiplication algorithms. In *International Conference on Computational Science*. Springer, 51–60.
- [20] Alexander Heinecke, Alexander Breuer, Michael Bader, and Pradeep Dubey. 2016. High order seismic simulations on the Intel Xeon Phi processor (Knights Landing). In *International Conference on High Performance Computing*. Springer, 343–362.
- [21] Alexander Heinecke, Greg Henry, Maxwell Hutchinson, and Hans Pabst. 2016. LIBXSMM: accelerating small matrix multiplications by runtime code generation. In *SC’16: Proceedings of the International Conference for High Performance Computing, Networking, Storage and Analysis*. IEEE, 981–991.
- [22] Alexander Heinecke, Hans Pabst, and Greg Henry. 2015. Libxsmm: A high performance library for small matrix multiplications. *Poster and Extended Abstract Presented at SC* (2015).
- [23] Changwan Hong, Aravind Sukumaran-Rajam, Israt Nisa, Kunal Singh, and P Sadayappan. 2019. Adaptive sparse tiling for sparse matrix multiplication. In *Proceedings of the 24th Symposium on Principles and Practice of Parallel Programming*. 300–314.
- [24] Andrew Howard, Mark Sandler, Grace Chu, Liang-Chieh Chen, Bo Chen, Mingxing Tan, Weijun Wang, Yukun Zhu, Ruoming Pang, Vijay Vasudevan, Quoc V. Le, and Hartwig Adam. 2019. Searching for MobileNetV3. In *The IEEE International Conference on Computer Vision (ICCV)*.
- [25] Aleksandar Ilic, Frederico Pratas, and Leonel Sousa. 2014. Cache-aware Roofline model: Upgrading the loft. *IEEE Computer Architecture Letters* 13, 1 (2014), 21–24.
- [26] R Intel. 2014. Intel 64 and ia-32 architectures optimization reference manual. *Intel Corporation, Sept* (2014).
- [27] François Irigoien and Rémi Triolet. 1988. Supernode partitioning. In *Proceedings of the 15th ACM SIGPLAN-SIGACT symposium on Principles of programming languages*. 319–329.
- [28] James Jeffers and James Reinders. 2013. *Intel Xeon Phi coprocessor high performance programming*. Newnes.
- [29] Zhen Jia, Aleksandar Zlateski, Fredo Durand, and Kai Li. 2018. Optimizing N-dimensional, winograd-based convolution for manycore CPUs. In *Proceedings of the 23rd ACM SIGPLAN Symposium on Principles and Practice of Parallel Programming*. 109–123.
- [30] Ziheng Jiang, Tianqi Chen, and Mu Li. 2018. Efficient deep learning inference on edge devices. *ACM SysML* (2018).
- [31] Ken Kennedy and John R Allen. 2001. *Optimizing compilers for modern architectures: a dependence-based approach*. Morgan Kaufmann Publishers Inc.
- [32] Daya Khudia, Protonu Basu, and Summer Deng. 2018. Open-sourcing FBGEMM for state-of-the-art server-side inference.
- [33] Fredrik Kjolstad, Shoaib Kamil, Stephen Chou, David Lugato, and Saman Amarasinghe. 2017. The tensor algebra compiler. *Proceedings of the ACM on Programming Languages* 1, OOPSLA (2017), 1–29.
- [34] Süreyya Emre Kurt, Aravind Sukumaran-Rajam, Fabrice Rastello, and Ponnuswamy Sadayappan. 2020. Efficient tiled sparse matrix multiplication through matrix signatures. In *SC20: International Conference for High Performance Computing, Networking, Storage and Analysis*. IEEE, 1–14.
- [35] Monica D Lam, Edward E Rothberg, and Michael E Wolf. 1991. The cache performance and optimizations of blocked algorithms. *ACM SIGOPS Operating Systems Review* 25, Special Issue (1991), 63–74.
- [36] Jakob Leben and George Tzanetakis. 2019. Polyhedral compilation for multi-dimensional stream processing. *ACM Transactions on Architecture and Code Optimization (TACO)* 16, 3 (2019), 1–26.
- [37] Michael Metcalf. 1980. *Fortran program optimization*. Technical Report. European Organization for Nuclear Research.
- [38] Jakob Nielsen. 1994. *Usability engineering*. Morgan Kaufmann.
- [39] Travis E Oliphant. 2006. *A guide to NumPy*. Vol. 1. Trelgol Publishing USA.
- [40] Neungsoo Park, Wenheng Liu, Viktor K Prasanna, and Cauligi Raghavendra. 2000. Efficient matrix multiplication using cache conscious data layouts. In *Prof. of HPCMO User Group Conference*.
- [41] Adam Paszke, Sam Gross, Francisco Massa, Adam Lerer, James Bradbury, Gregory Chanan, Trevor Killeen, Zeming Lin, Natalia Gimelshein, Luca Antiga, Alban Desmaison, Andreas Kopf, Edward Yang, Zachary DeVito, Martin Raison, Alykhan Tejani, Sasank Chilamkurthy, Benoit Steiner, Lu Fang, Junjie Bai, and Soumith Chintala. 2019. PyTorch: An Imperative Style, High-Performance Deep Learning Library. In *Advances in Neural Information Processing Systems* 32, H. Wallach, H. Larochelle, A. Beygelzimer, F. d’Alché-Buc, E. Fox, and R. Garnett (Eds.). Curran Associates, Inc., 8024–8035. <http://papers.neurips.cc/paper/9015-pytorch-an-imperative-style-high-performance-deep-learning-library.pdf>
- [42] Jonathan Ragan-Kelley, Connelly Barnes, Andrew Adams, Sylvain Paris, Frédo Durand, and Saman Amarasinghe. 2013. Halide: a language and compiler for optimizing parallelism, locality, and recomputation in image processing pipelines. *Acm Sigplan Notices* 48, 6 (2013), 519–530.
- [43] MMG Ricci and Tullio Levi-Civita. 1900. Méthodes de calcul différentiel absolu et leurs applications. *Math. Ann.* 54, 1-2 (1900), 125–201.
- [44] Alexander Rush. 2018 (accessed August 26, 2020). *Tensor Considered Harmful*. <http://nlp.seas.harvard.edu/NamedTensor>
- [45] Tyler M Smith, Robert Van De Geijn, Mikhail Smelyanskiy, Jeff R Hammond, and Field G Van Zee. 2014. Anatomy of high-performance many-threaded matrix multiplication. In *2014 IEEE 28th International Parallel and Distributed Processing Symposium*. IEEE, 1049–1059.
- [46] Daniele G Spampinato and Markus Püschel. 2014. A basic linear algebra compiler. In *Proceedings of Annual IEEE/ACM International Symposium on Code Generation and Optimization*. 23–32.
- [47] Paul Springer and Paolo Bientinesi. 2018. Design of a high-performance gemm-like tensor-tensor multiplication. *ACM Transactions on Mathematical Software (TOMS)* 44, 3 (2018), 1–29.

- [48] Benoit Steiner, Chris Cummins, Horace He, and Hugh Leather. 2021. Value learning for throughput optimization of deep learning workloads. *Proceedings of Machine Learning and Systems* 3 (2021).
- [49] Benoit Steiner, Chris Cummins, Horace He, and Hugh Leather. 2021. Value Learning for Throughput Optimization of Deep Neural Networks.
- [50] Harold S Stone. 1970. A logic-in-memory computer. *IEEE Trans. Comput.* 100, 1 (1970), 73–78.
- [51] Field G Van Zee and Robert A Van De Geijn. 2015. BLIS: A framework for rapidly instantiating BLAS functionality. *ACM Transactions on Mathematical Software (TOMS)* 41, 3 (2015), 1–33.
- [52] Endong Wang, Qing Zhang, Bo Shen, Guangyong Zhang, Xiaowei Lu, Qing Wu, and Yajuan Wang. 2014. Intel math kernel library. In *High-Performance Computing on the Intel® Xeon Phi™*. Springer, 167–188.
- [53] Wikipedia. 2020. Instruction pipelining — Wikipedia, The Free Encyclopedia. <http://en.wikipedia.org/w/index.php?title=Instruction%20pipelining&oldid=1070706552>. [Online; accessed 29-August-2020].
- [54] Wikipedia. 2020. Loop unrolling — Wikipedia, The Free Encyclopedia. <http://en.wikipedia.org/w/index.php?title=Loop%20unrolling&oldid=1080086803>. [Online; accessed 29-August-2020].
- [55] Wikipedia contributors. [n.d.]. Plagiarism — Wikipedia, The Free Encyclopedia. https://en.wikipedia.org/wiki/Loop_nest_optimization#Example:_matrix_multiplication [Online; accessed 15-November-2021].
- [56] Samuel Williams, David Patterson, Leonid Oliker, John Shalf, and Katherine Yelick. 2008. The roofline model: A pedagogical tool for auto-tuning kernels on multicore architectures. In *Hot Chips*, Vol. 20. 24–26.
- [57] Michael E Wolf and Monica S Lam. 1991. A data locality optimizing algorithm. In *Proceedings of the ACM SIGPLAN 1991 conference on Programming language design and implementation*. 30–44.
- [58] Michael Wolfe. 1989. More iteration space tiling. In *Proceedings of the 1989 ACM/IEEE conference on Supercomputing*. 655–664.
- [59] Ruizhe Zhao, Shuanglong Liu, Ho-Cheung Ng, Erwei Wang, James J Davis, Xinyu Niu, Xiwei Wang, Huifeng Shi, George A Constantinides, Peter YK Cheung, et al. 2018. Hardware compilation of deep neural networks: An overview. In *2018 IEEE 29Th international conference on application-specific systems, architectures and processors (ASAP)*. IEEE, 1–8.
- [60] Lanmin Zheng and Tianqi Chen. 2018. Optimizing deep learning workloads on ARM GPU with TVM. In *Proceedings of the 1st on Reproducible Quality-Efficient Systems Tournament on Co-Designing Pareto-Efficient Deep Learning*. 1.
- [61] Lianmin Zheng, Chengfan Jia, Minmin Sun, Zhao Wu, Cody Hao Yu, Ameer Haj-Ali, Yida Wang, Jun Yang, Danyang Zhuo, Koushik Sen, et al. 2020. Ansor: Generating High-Performance Tensor Programs for Deep Learning. *arXiv preprint arXiv:2006.06762* (2020).
- [62] Aleksandar Zlateski, Zhen Jia, Kai Li, and Fredo Durand. 2018. A Deeper Look at FFT and Winograd Convolutions.
- [63] Aleksandar Zlateski, Zhen Jia, Kai Li, and Fredo Durand. 2019. The anatomy of efficient FFT and winograd convolutions on modern CPUs. In *Proceedings of the ACM International Conference on Supercomputing*. 414–424.
- [64] Aleksandar Zlateski and H Sebastian Seung. 2017. Compile-time optimized and statically scheduled ND convnet primitives for multi-core and many-core (Xeon Phi) CPUs. In *Proceedings of the International Conference on Supercomputing*. 1–10.